Three-parameter Kerr soil model: finite element formulation and applications in transient dynamic analyses

Luiz Antonio Farani de Souza[1]*, Sara Coelho da Silva[2]

[1] lasouza@utfpr.edu.br. Federal Technological University of Paraná (UTFPR), Apucarana, Paraná, Brazil. ORCID: https://orcid.org/0000-0001-7194-5851
[2] sarasilva@utfpr.edu.br. Federal Technological University of Paraná (UTFPR), Campo Mourão, Paraná, Brazil. ORCID: https://orcid.org/0000-0003-3530-1914
* corresponding author

Abstract
Soil-structure interaction is a topic of paramount importance in civil engineering, as the method of soil modeling directly influences the static and dynamic performance of structures supported by elastic foundations. Simplified models, such as Winkler's, while widely adopted, fail to adequately represent the effects of distributed stiffness and lateral interaction. In this context, multiparameter models, like those proposed by Pasternak and Kerr, offer a more realistic characterization of soil behavior. This work aims to develop and implement the explicit formulation of the stiffness matrix for Kerr's soil model, based on the Finite Element Method, and apply it to transient dynamic analyses of beams. The methodology employs Euler-Bernoulli beam finite elements with two nodes and four degrees of freedom, discretized mass in condensed form, and mass-proportional damping. The equation of motion is solved using the Backward Acceleration Method, an implicit, symplectic, and energy-conserving temporal integration scheme. Three dynamic problems involving beams on elastic foundations are analyzed: a free-ended beam subjected to a concentrated moment, a simply supported beam under variable dynamic loading, and a cantilever beam under a concentrated force. In all cases, the performance of Winkler, Pasternak, and Kerr soil models is compared. The principal results indicate that the Winkler model leads to larger displacements and lower frequencies due to its simplified formulation. The Pasternak model, by incorporating lateral interaction, reduces oscillation amplitudes and periods. The Kerr model, conversely, exhibits the most rigid response, with smaller displacements and higher natural frequencies. Comparison with literature results confirms the validity of the proposed model, highlighting its applicability in dynamic analyses of beams on elastic foundations.
Keywords: dynamic analysis; elastic foundation; finite elements; Kerr model; soil-structure interaction.

Modelo de solo de Kerr com três parâmetros: formulação em elementos finitos e aplicações em análises dinâmicas transientes

Resumo
A interação solo-estrutura é um tema de grande relevância em engenharia civil, porque a forma como o solo é modelado influencia diretamente o desempenho estático e dinâmico de estruturas apoiadas em fundações elásticas. Modelos simplificados, como o de Winkler, embora amplamente utilizados, não representam adequadamente os efeitos de rigidez distribuída e de interação lateral. Nesse contexto, modelos com multiparâmetros, como os de Pasternak e Kerr, oferecem uma caracterização mais realista do comportamento do solo. O objetivo deste trabalho é desenvolver e implementar a formulação explícita da matriz de rigidez do modelo de solo de Kerr, fundamentada no Método dos Elementos Finitos, e aplicá-la em análises dinâmicas transientes de vigas. A metodologia considera elementos finitos de viga de Euler-Bernoulli com dois nós e quatro graus de liberdade, massa discretizada em forma condensada e amortecimento proporcional à massa. A equação de movimento é resolvida pelo Método de Aceleração Regressiva, um esquema de integração temporal implícito e conservativo de energia. Três problemas dinâmicos de vigas sobre fundações elásticas são analisados:

Early View

viga com extremidades livres submetida a momento concentrado, viga biapoiada sob carregamento dinâmico variável e viga em balanço sujeita à força concentrada. Em todos os casos, compara-se o desempenho dos modelos de solo de Winkler, Pasternak e Kerr. Os principais resultados mostram que o modelo de Winkler conduz a maiores deslocamentos e menores frequências, devido à sua formulação simplificada. O modelo de Pasternak, ao incluir a interação lateral, reduz amplitudes e períodos de oscilação. Já o modelo de Kerr apresenta a resposta mais rígida, com menores deslocamentos e frequências naturais mais elevadas. A comparação com resultados da literatura confirma a validade do modelo proposto, destacando sua aplicabilidade em análises dinâmicas de vigas sobre fundações elásticas.
Palavras-chave: *análise dinâmica; elementos finitos; fundação elástica; interação solo-estrutura; modelo de Kerr.*

1 Introduction

The interaction between beams and slabs and the supporting soil is a classic scenario in engineering, often classified as a Soil-Structure Interaction (SSI) problem (Worku; Habte, 2022). This area of study is notably complex because it integrates knowledge from various disciplines, such as soil and structural dynamics, earthquake engineering (or seismic engineering), geomechanics, geophysics, and materials science. The success achieved in SSI investigations has driven the continuous development of new theories, methodologies, and experimental configurations. Thanks to technological advancements, the field of SSI analysis has expanded considerably. Currently, a variety of approaches are employed, including analytical methods, numerical methods, hybrid techniques (analytical-numerical), in addition to practical experiments and the direct observation of prototypes. This diversity of tools allows for a deeper and more precise understanding of the behavior of structures in contact with the soil (Mourya *et al*., 2023).

The analysis and design of an adequate foundation are fundamental for any civil engineering work. The structure's loads, encompassing both its self-weight and external loads (or live loads), are transmitted to the soil by the foundation. The settlement of the soil can generate additional deformations and stresses in the building's superstructure. Frequently, the superstructure analysis is simplified by assuming its base is perfectly fixed to the ground (Pandey *et al*., 2023).

Foundations are essential components in various physical systems, with applications in fields as varied as mechanical, civil, and electrical engineering, nanotechnology, and even biotechnology. Due to their critical importance, they are a constant focus of research, especially regarding their dynamic behavior. The primary function of foundations is to protect a structure against oscillations and, thus, prevent mechanical failure. For this reason, engineers and researchers must follow three crucial steps in designing any system subjected to vibrations. First, it is necessary to create a continuous model for the structure. Next, it is essential to develop a mathematical model for the foundation. Finally, the design must integrate a comprehensive model that considers the interaction between the foundation and the structure it supports (Younesian *et al*., 2019).

The problem of beams on a flexible foundation is considered a classic example where the mechanics of interaction between the beams and the foundation plays an essential role in system modeling. Generally, mathematical models for representing foundation flexibility can be grouped into two categories: the continuum model and the spring model. In the continuum model, foundation flexibility is accounted for by considering the foundation as a homogeneous semi-infinite elastic body. Conversely, in the spring model, foundation flexibility is considered by treating it as a set of continuous springs (Limkatanyu *et al*., 2013).

Regarding foundation modeling, the Winkler model is notable for its simplicity. It represents the soil as a series of discrete, independent springs, which allows for the description of its behavior under compression. For this reason, this model is widely used in SSI analysis. However, the Winkler foundation model does not consider the shear force transfer between adjacent regions of the soil (Karkon; Karkon, 2016).

Early View

Researchers have developed multiparameter foundation models to consider SSI, such as the Vlasov foundation model (Wang; Zhou; Wang, 2022) and the Pasternak foundation model (Guellil *et al*., 2021). The three-parameter model proposed by Kerr (Kerr, 1965) is an evolution of the Pasternak model (Pasternak, 1954). It adds a layer of springs, which solves the problem of concentrated reactions or infinite reaction pressures, and also allows for the specification of an additional boundary condition for the constraints in the foundation. In some cases, this boundary condition can significantly influence the structure's behavior. For these reasons, the Kerr foundation model has been widely used in analyses to study the impact of geometric parameters of slabs and/or beams, made of various materials, and the soil stiffness on deformation, vibration, and wave propagation (Dai *et al*., 2025).

To enhance the design of structural foundations, there is a continuous effort to improve how the soil is modeled and how its interaction with the structure is simulated. This soil-structure interaction is crucial and challenging to represent accurately, both concerning the soil and the structure's behavior. This type of contact is frequent in civil engineering, occurring in foundations, railway tracks (or railroads), underground pipelines, retaining walls, and tunnels, among other applications. These scenarios are classified as contact problems, which can be bilateral or unilateral in nature. Bilateral contact assumes the contact medium responds to both tensile and compressive forces. However, a more faithful representation of soil behavior is achieved by considering that it reacts only to compressive forces, which defines the contact as unilateral (Rosas; Silva; Silveira, 2018).

The central objective of this work is to present the development and explicit formulation of the stiffness matrix associated with the Kerr foundation model, which stands out for incorporating three parameters and enabling a more comprehensive representation of soil-structure interactions. Beyond the theoretical derivation, the methodological proposal includes the computational implementation of the model and its application in transient dynamic analyses of beams, allowing the structural behavior to be evaluated under different elastic foundation conditions.

The numerical model developed for the analysis of beams on an elastic base is based on the Finite Element Method (FEM), adopting the classical Euler-Bernoulli beam theory and considering assumptions of geometric and material linearity. For foundation representation, three established models from the literature were incorporated: the Winkler model, which describes the soil as independent linear springs; the Pasternak model, which adds a shear parameter to represent the lateral interaction between springs; and the Kerr model, which extends Pasternak's by introducing a third parameter associated with an additional rigid layer, enabling a more realistic characterization of the soil-structure interaction.

The discretization of the structures is performed using two-node beam finite elements with a total of four degrees of freedom (two translations and two rotations), ensuring a formulation suitable for static and dynamic analyses. The mass matrix adopted in the simulations is the lumped (or condensed) form, where the structure's mass is concentrated at the nodes. This simplification generates a diagonal matrix, which facilitates numerical treatment and reduces the computational cost. The representation of structural damping is done through a mass-proportional damping matrix, where energy dissipation is modeled in a simplified manner as a proportion of the structural inertia.

The equation of motion of the discrete system is solved using the Backward Acceleration Method (Liu; Li; Zhao, 2013), which belongs to the Newmark family of methods, with parameters $\beta = \gamma = 1/2$. This is an implicit and energy-conservative time integration method, making it suitable for long-duration transient dynamic analyses. Its formulation ensures numerical stability, requires only the resolution of a system of linear equations per time step, and preserves the symmetry properties of the effective stiffness matrix, favoring computational processing efficiency. The numerical model is applied in three numerical examples of dynamic analysis of beams on elastic foundations using the Scilab software, version 2025.1.0 (Dassault Systemes, 2025), with the objective of evaluating the influence of different soil models on the structural response.

The justification for the development of the present investigation is related to the need for more realistic soil models for the design and analysis of structural systems supported on elastic foundations. Simplified models, although widely used, do not adequately capture the effects of distributed stiffness and lateral interaction that can be decisive in structural performance. In this regard, by providing a

Early View

rigorous and validated formulation of the Kerr model, the article offers theoretical and practical support for safer and more efficient designs, in addition to paving the way for future studies that explore the influence of different soil parameters in static and dynamic analyses.

The remainder of this paper is organized as follows. Section 2 presents the theoretical framework, including the formulation of the three-parameter Kerr soil model, the equation of motion and the Backward Acceleration Method, as well as the mass and damping matrices. Section 3 describes the research methodology, including the finite element discretization, the implementation of the Winkler, Pasternak, and Kerr foundation models, and the numerical procedures adopted for the transient and modal analyses. Section 4 presents and discusses three numerical examples involving beam with free ends, simply supported beam, and cantilever beam, highlighting the influence of the soil model on the static and dynamic structural responses and comparing the results with available literature data. Finally, Section 5 summarizes the main findings, discusses the limitations of the proposed formulation, and outlines potential directions for future research.

2 Theoretical framework

This section presents the conceptual and mathematical fundamentals that underpin the proposed numerical model. Initially, the three-parameter formulation of the Kerr soil model is developed. Subsequently, the equation of motion used in the dynamic analysis of structures is described, with emphasis on the application of the Backward Acceleration Method. The mass and damping matrices are also addressed. Finally, the computational implementation of the elastic foundation model within a finite element environment is detailed, which serves as the basis for the transient dynamic analyses conducted throughout this study.

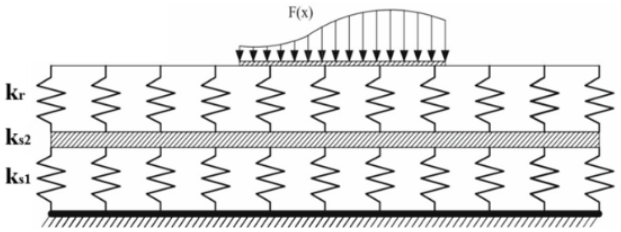
2.1 Kerr soil model

The three-layer model proposed by Kerr (1965) is an extension of the Pasternak model. This model considers the soil as a system of two layers of springs (k_{s1} and k_r) coupled by a shear layer (k_{s2}) (Avramidis; Morfidis, 2006; Pandey *et al*., 2023). The strain energy of the soil-U-beam system presented in Brito (2024) can be described by:

$$U = \frac{1}{2}\int_0^L \left[k_{s1} v(x)^2 + k_{s2}\left(\frac{dv(x)}{dx}\right)^2 + k_r\left(\frac{d^2v(x)}{dx^2}\right)^2 \right] dx \tag{1}$$

where $v(x)$ is the vertical displacement of the beam and L is the element length. The Kerr-type foundation model is illustrated in Figure 1.

Figure 1 – Kerr-type soil model



Source: adapted from Younesian *et al*. (2019).

Applying the Finite Element Method, the displacement $v(x)$ is interpolated using shape functions described in Kwon and Bang (2018) as follows:

$$v(x) = \sum_{i=1}^{4} N_i(x) a_i = N_1(x)a_1 + N_2(x)a_2 + N_1(x)a_3 + N_2(x)a_4 \tag{2}$$

Early View

where $a = \left[v_1\ \theta_1\ v_2\ \theta_2\ \right]^T$ is the nodal displacement vector. For an Euler-Bernoulli beam element with two nodes (four degrees of freedom: two translations and two rotations), the shape functions N_i are given by:

$$N = \left[N_1\ N_2\ N_3\ N_4\ \right]^T \tag{3}$$

where

$$N_1 = 1 - 3\ ^2 + 2\ ^3 \tag{4}$$

$$N_2 = L\left(-\ 2\ ^2 +\ ^3\right) \tag{5}$$

$$N_3 = 3\ ^2 - 2\ ^3 \tag{6}$$

$$N_4 = L\left(-\ ^2 +\ ^3\right) \tag{7}$$

where $= x/L$. The derivatives are given by the vectors B_1 and B_2:

$$B_1 = \frac{dN}{dx} = \frac{d}{dx}\frac{dN}{d} = \frac{1}{L}\frac{dN}{d} \tag{8}$$

$$B_1 = \frac{1}{L}\left[-\ 6 + 6\ ^2\ L\left(1 - 4 + 3^2\right)\ 6 - 6\ ^2\ L\left(-\ 2 + 3\ ^2\right)\right]^T \tag{9}$$

$$B_2 = \frac{d^2N}{dx^2} = \frac{1}{L^2}\frac{d^2N}{d\ ^2} \tag{10}$$

$$B_2 = \frac{1}{L^2}\left[-\ 6 + 12\ L(-\ 4 + 6)\ 6 - 12\ L(-\ 2 + 6)\right]^T \tag{11}$$

where $d/dx = 1/L$. The soil stiffness matrix K_s for the Kerr soil model is obtained by the discretization of the strain energy U:

$$K_s = \int_0^L \left(k_{s1} N N^T + k_{s2} B_1 B_1^T + k_r B_2 B_2^T\right) dx = K_{s1} + K_{s2} + K_r \tag{12}$$

The soil stiffness matrix K_s is then calculated numerically via Gauss-Legendre integration. The vertical stiffness contribution matrix K_{s1} (Winkler soil model) for the finite element is given by (Teodoru; Muşat, 2008):

$$K_{s1} = k_{s1}\int_0^L NN^T dx = \frac{k_{s1}L}{420}\left[156\ 22L\ 22L\ 4L^2\ 54\ -\ 13L\ 13L\ -\ 3L^2\ 54\ 13L\ -\ 13L\right. \tag{13}$$

The shear stiffness matrix K_{s2} is described by:

$$K_{s2} = k_{s2}\int_0^L B_1 B_1^T dx = \frac{k_{s2}}{30L}\left[36\ 3L\ 3L\ 4L^2\ -\ 36\ 3L\ -\ 3L\ -\ L^2\ -\ 36\ -\ 3L\ 3L\ \cdot\right. \tag{14}$$

Early View

The matrix referring to the interaction parameter (K_r) is written as follows:

$$K_r = k_r \int_0^L B_2 B_2^T dx = \frac{k_r}{L^3}\left[12\ 6L\ 6L\ 4L^2\ -12\ 6L\ -6L\ 2L^2\ -12\ -6L\ 6L\ 2L^2\ 12\right. \quad (15)$$

Setting $= x/L$ in the elements of the vector B_2, the terms of the matrix in Equation 15 are determined as follows:

$$K_r(1,1) = \frac{k_r}{L^4}\int_0^L \left(-6 + 12\frac{x}{L}\right)^2 dx = \frac{12k_r}{L^3} \quad (16)$$

$$K_r(2,2) = \frac{k_r}{L^4}\int_0^L L^2\left(-4 + 6\frac{x}{L}\right)^2 dx = \frac{4k_r}{L} \quad (17)$$

$$K_r(3,3) = \frac{k_r}{L^4}\int_0^L \left(6 - 12\frac{x}{L}\right)^2 dx = \frac{12k_r}{L^3} \quad (18)$$

$$K_r(4,4) = \frac{k_r}{L^4}\int_0^L L^2\left(-2 + 6\frac{x}{L}\right)^2 dx = \frac{4k_r}{L} \quad (19)$$

$$K_r(1,2) = K_r(2,1) = \frac{k_r}{L^4}\int_0^L L\left(-6 + 12\frac{x}{L}\right)\left(-4 + 6\frac{x}{L}\right)dx = \frac{6k_r}{L^2} \quad (20)$$

$$K_r(1,3) = K_r(3,1) = \frac{k_r}{L^4}\int_0^L \left(-6 + 12\frac{x}{L}\right)\left(6 - 12\frac{x}{L}\right)dx = \frac{-12k_r}{L^3} \quad (21)$$

$$K_r(1,4) = K_r(4,1) = \frac{k_r}{L^4}\int_0^L L\left(-6 + 12\frac{x}{L}\right)\left(-2 + 6\frac{x}{L}\right)dx = \frac{6k_r}{L^2} \quad (22)$$

$$K_r(2,3) = K_r(3,2) = \frac{k_r}{L^4}\int_0^L L\left(-4 + 6\frac{x}{L}\right)\left(6 - 12\frac{x}{L}\right)dx = \frac{-6k_r}{L^2} \quad (23)$$

$$K_r(3,4) = K_r(4,3) = \frac{k_r}{L^4}\int_0^L L\left(6 - 12\frac{x}{L}\right)\left(-2 + 6\frac{x}{L}\right)dx = \frac{-6k_r}{L^2} \quad (24)$$

$$K_r(2,4) = K_r(4,2) = \frac{k_r}{L^4}\int_0^L L^2\left(-4 + 6\frac{x}{L}\right)\left(-2 + 6\frac{x}{L}\right)dx = \frac{2k_r}{L} \quad (25)$$

The elementary stiffness matrix of the beam element in the local coordinate system is given by (Kwon; Bang, 2018):

$$K_M = \frac{E}{L}\left[12c_1\ 6c_2\ 6c_2\ 4I\ -12c_1\ 6c_2\ -6c_2\ 2I\ -12c_1\ -6c_2\ 6c_2\ 2I\ 12c_1\ -6c_2\right. \quad (26)$$

where $c_1 = \frac{I}{L^2}$, and $c_2 = \frac{I}{L}$. In Equation 26, E is the longitudinal modulus of elasticity, and I is the moment of inertia. In the classical Euler-Bernoulli theory, planes normal to the neutral axis of the beam remain straight and normal after deformation (Avramidis; Morfidis, 2006). Thus, the finite element stiffness matrix of the beam with the Kerr soil model is described by:

$$K_e = K_M + K_s = K_M + K_{s1} + K_{s2} + K_r \quad (27)$$

Early View

2.2 Equation of motion and solution method

The dynamic response of structures is often obtained by solving the equation of motion (Chen *et al.*, 2022):

$$Ku + C\dot{u} + M\ddot{u} = F_{ext} \tag{28}$$

where M, C, and K, respectively, the mass, damping, and stiffness matrices of the structural system; F_{ext} is the applied load vector; and u, $\dot{u}$, and $\ddot{u}$ are, respectively, the displacement, velocity, and acceleration vectors.

An iterative method, belonging to the Newmark family (with $\beta = \gamma = 1/2$) and titled the Backward Acceleration Method, was developed by Liu, Li, and Zhao (2013) to solve initial value problems in FEM simulations. This method, which is classified as a symplectic time integration method, has as its main advantage the conservation of the system's total energy. Only one set of implicit equations needs to be solved at each time step, which simplifies the computation. The effective stiffness matrix and the effective load vector are symmetric, which optimizes the solution. In terms of efficiency, the method is as effective as the trapezoidal rule because both require the same computational effort. Furthermore, this approach does not introduce artificial variables or parameters, making it more direct and robust. The displacement vector u at the current time step ($t + \Delta t$) is determined by:

$$t + \Delta tu = tu + t\,t\dot{u} + \frac{t^2}{2}t + \Delta t\ddot{u} \tag{29}$$

where t is the time step, the left superscript (t) indicates the previous time step, and the right superscript (k) indicates the previous iteration. The effective load vector $t + \Delta tF_{ef}^{(k+1)}$ and the effective stiffness matrix $t + \Delta tK_{ef}^{(k+1)}$, respectively, at the current iteration ($k + 1$) are mathematically expressed by:

$$t + \Delta tF_{ef}^{(k+1)} = F_{int}\left(t + \Delta tu^{(k)}\right) + \frac{2}{t^2}t + \Delta tM\,t + \Delta tu^{(k)} - t + \Delta tM\,t + \Delta tq_s + \tag{30}$$

$$t + \Delta tK_{ef}^{(k+1)} = K\left(t + \Delta tu^{(k)}\right) + \frac{2}{t^2}t + \Delta tM + \frac{1}{t}t + \Delta tC \tag{31}$$

where the vectors $t + \Delta tq_s$ and $t + \Delta tr_s$ represent the dynamic contributions at the current time and are, respectively, given by:

$$t + \Delta tq_s = \frac{2}{t^2}tu + \frac{2}{t}t\dot{u} \tag{32}$$

$$t + \Delta tr_s = t\dot{u} + \frac{t}{2}t\ddot{u} \tag{33}$$

The iterative equations that establish the dynamic equilibrium of the structural system as a function of the displacement variable u are:

$$t + \Delta tK_{ef}^{(k+1)}\,t + \Delta t\delta u^{(k+1)} = -\,t + \Delta tF_{ef}^{(k+1)} \tag{34}$$

$$t + \Delta tu^{(k+1)} = t + \Delta tu^{(k)} + t + \Delta t\delta u^{(k+1)} \tag{35}$$

Early View

The velocity vector $t + \Delta t\dot{u}$ and acceleration vector $t + \Delta t\ddot{u}$ at the current time step are, respectively, given by:

$$t + \Delta t\dot{u} = \frac{1}{t}t + \Delta tu + t + \Delta tr_s - \frac{t}{2}t + \Delta tq_s \tag{36}$$

$$t + \Delta t\ddot{u} = \frac{2}{t^2}t + \Delta tu - t + \Delta tq_s \tag{37}$$

2.3 Mass matrix

The mass matrix can be lumped (also called condensed or diagonal) or consistent. In the former, a simplified procedure is adopted that concentrates the mass at the nodal points. The advantage of this technique is the generation of a diagonal matrix, which simplifies the numerical treatment. The latter is obtained through the Finite Element Method formulation. Defining the mass per unit length of a straight bar with constant cross-section as $\mu = \rho A$, the elementary lumped mass matrix M_e in the local Cartesian coordinate system is presented as (Soriano, 2014):

$$M_e = \frac{\mu L}{2} diag[1 \ \frac{L^2}{12} \ 1 \ \frac{L^2}{12}] \tag{38}$$

where the symbol *diag*[…] represents a diagonal matrix with the diagonal coefficients shown inside the brackets. Although the lumped mass matrix is adopted due to its simplicity and computational efficiency, it is important to emphasize that the use of a consistent mass matrix can improve the accuracy of the dynamic response. The consistent mass formulation provides a more faithful representation of the distributed inertia along the structure, which directly affects the accuracy of the computed natural frequencies, particularly for higher vibration modes, as these are more sensitive to the adopted discretization method. The inclusion of this formulation would enable the assessment of the sensitivity of the dynamic response and the comparison of numerical errors at high frequencies, considering that consistent and lumped mass formulations typically provide upper and lower bounds for the eigenvalues, respectively (Chopra, 2020; Soriano, 2014).

2.4 Damping matrix

Vibrational energy in structures is dissipated by various mechanisms, such as thermal effects caused by the repetition of stress cycles, internal friction associated with material deformation, and friction at the connections between elements. In structural applications, the dissipation mechanisms vary according to the material properties and the interactions between their components. The precise mathematical formulation of this dissipation is complex and generally difficult to estimate, which is why simplified damping models are often used (Cimellaro; Marasco, 2018). Structural damping is a measure of energy dissipation that leads the structure from a vibratory state to a state of rest. In the dynamic analysis of beams, a simple way to represent energy dissipation is through mass-proportional damping. In this model, the damping matrix C is proportional to the mass matrix M, without a stiffness contribution. The damping matrix is mathematically described by (Fernandes; Vasconcellos; Greco, 2018):

$$C = 2\, c_m M \tag{39}$$

where c_m is the scalar coefficient that defines the intensity of the energy dissipation. The use of mass-proportional damping introduces dissipative forces that depend exclusively on the inertia distribution, making it a simple, single-parameter model that ensures numerical stability in time integration methods like Newmark's. It is particularly suitable for transient analyses where the response is governed by low-frequency modes. However, its application must be judicious. The model

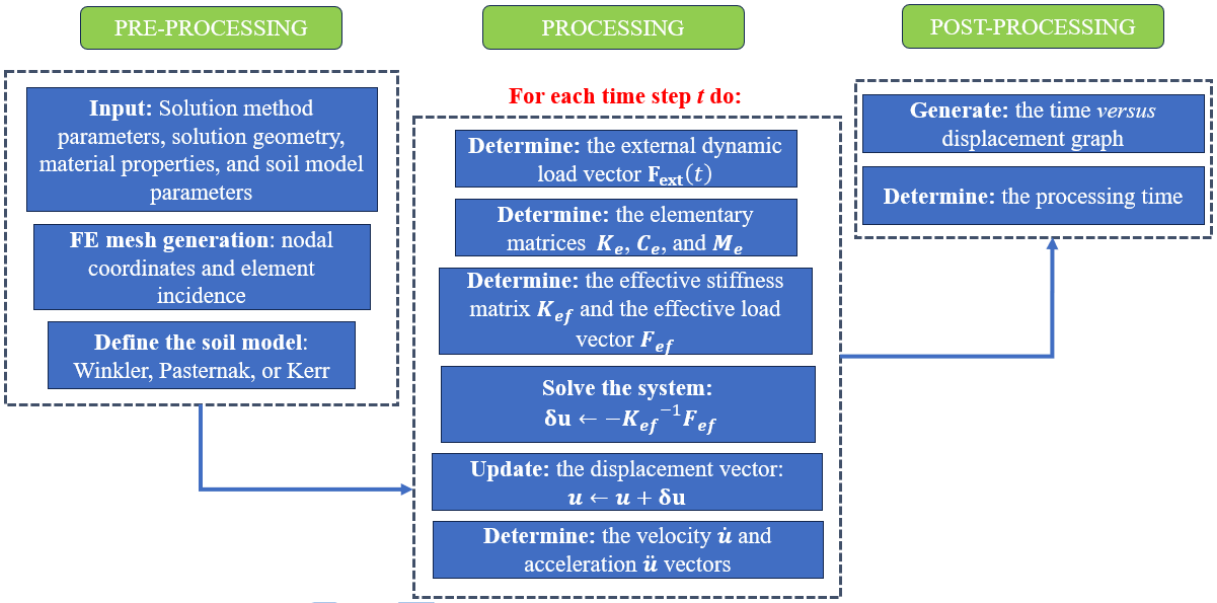
Early View

tends to underestimate energy dissipation at higher frequencies, meaning that in structures sensitive to high-frequency vibrations, improper calibration of the scalar coefficient can yield distorted responses with unrealistic stresses and displacements. To avoid compromising the analysis accuracy in such cases, it is recommended to adopt more comprehensive approaches, such as Rayleigh proportional damping, which provide a realistic representation of damping effects distributed over broader frequency ranges (Chopra, 2020; Craig Jr.; Kurdila, 2006).

3 Research methodology

The structures are discretized using the Finite Element Method (FEM), employing two-node beam finite elements with a total of four degrees of freedom, considering the Euler-Bernoulli beam theory and coupled to the Winkler, Pasternak, and Kerr type soil models. The program was developed in the Scilab environment, version 2025.1.0 (Dassault Systemes, 2025), structured modularly, allowing any of the soil models to be selected. The flowchart containing the steps for the numerical solution is described in Figure 2.

Figure 2 – Flowchart of the steps for the transient analysis



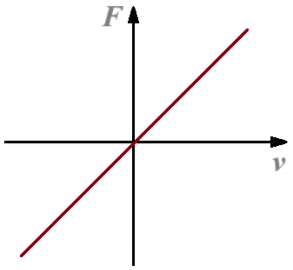
Source: elaborated by the authors.

In the structural analyses of the soil-structure interaction problems, assumptions of geometric linearity and material linearity are considered. The deformations are small enough that the deformed geometry does not significantly alter the equilibrium or the stiffness of the structure. The materials follow the linear elastic constitutive law (Hooke's Law).

The soil parameters considered for each model are: Winkler (k_{s1}), Pasternak (k_{s1} and k_{s2}), and Kerr (k_{s1}, k_{s2}, and k_r). The soil-structure interaction is treated as bilateral. The bilateral contact considers that the soil reacts to both tensile and compressive stresses/demands. In this case, it is assumed that the soil works fully connected to the structure, with no loss of contact occurring (Rosas; Silva; Silveira, 2018). Although the analyses consider a bilateral contact approach, real geotechnical systems often exhibit unilateral contact behavior. In practice, the soil is unable to sustain tensile stresses, which may lead to partial or total loss of contact (gap formation) between the structure and the supporting medium under certain loading conditions. This phenomenon can significantly affect the structural response, particularly in dynamic problems involving uplift or cyclic loading. Therefore, the assumption of fully bonded contact represents a simplification of the physical problem and may limit the applicability of the proposed model in scenarios where separation effects are relevant (Attar;

Karrech; Regenauer-Lieb, 2016; Silveira; Pereira; Gonçalves, 2008). The constitutive relation of force F versus displacement v of the soil, depicted by the graph in Figure 3, is linear and indicates that the soil stiffness remains constant.

Figure 3 – Force versus displacement relation of the linear bilateral foundation



Source: adapted from Rosas, Silva and Silveira (2018).

The Winkler foundation model is based on the assumption that the reaction at each point is proportional to the displacement at that point, and the springs are linear and independent (Younesian *et al.*, 2019). The stiffness matrix of the beam finite element with the Winkler soil model is represented by $K_e = K_M + K_{s1}$, by setting the matrices $K_{s2} = 0$ and $K_r = 0$ in Equation 27.

The Pasternak model formulation is an extension of the classic Winkler model, incorporating the interaction between the soil springs through a shear layer (K_{s2}). The stiffness matrix of the beam finite element with the Pasternak soil model is given by $K_e = K_M + K_{s1} + K_{s2}$, which implies $K_r = 0$ in Equation 27.

In Scilab, the solution of systems of linear equations is performed using matrix operators. In solving the system of linear equations described by Equation 34, the "backslash" operator ("\") is employed, which solves linear systems of the form $u = -K_{ef} \backslash F_{ef}$. The "\" operator is robust for well-conditioned systems. If the matrix is ill-conditioned (for example, with errors in the definition of constraints or improperly free degrees of freedom), Scilab generates a "Singular matrix" error or unstable solutions.

Natural frequencies are inherent properties of the structural system and depend on the mass and stiffness distribution of this system. Disregarding the effect of damping ($C = 0$), the equation of motion of the structural system in free vibration ($F_{ext} = 0$) is written according to Equation 40 (Chung; Yoo, 2002; Souza, 2024).

$$K\,u + M\,\ddot{u} = 0 \tag{40}$$

A possible solution for Equation 40 is of the form $u = \phi e^{i\omega t}$, which results in the classic eigenvalue and eigenvector problem given by the following expression:

$$K\phi e^{i\omega t} + M\,\phi\, i^2 \omega^2 e^{i\omega t} = 0, \tag{41}$$

where $i = \sqrt{-1}$, ϕ is the eigenvector corresponding to the mode shape (or mode of vibration), and ω is the eigenvalue that represents the square of a natural frequency of vibration of the structural system, given in rad/s. If the inverse of the matrix M exists (such that $M^{-1}M = I$) and multiplying both sides of Equation 41 by M^{-1}, it can be rewritten in the following form:

$$M^{-1}K\phi e^{i\omega t} = M^{-1}M\,\phi\,\omega^2 e^{i\omega t} \tag{42}$$

Early View

$$M^{-1}K\phi = I\phi\,\omega^2 \quad (43)$$

$$A\phi = \phi \quad (44)$$

where $A = M^{-1}K$ and $= \omega^2$. In the literature, there are computational algorithms capable of solving the problem given by Equation 44 and of providing, all at once, all the natural frequencies and their respective mode shapes. The number of mode shapes is equal to the number of degrees of freedom (DOF) of the structural system.

The Scilab function *[R, diagevals] = spec(A)* is used, where *R* is the eigenvector matrix and *diagevals* is the matrix containing the eigenvalues. This function uses two output arguments according to the syntax shown in Figure 4. Scilab uses, by default, algorithms based on the Schur decomposition to find the eigenvalues. The calculations are performed through optimized routines from the LAPACK library, which is a reference in numerical linear algebra.

Figure 4 – Code lines for the calculation of natural frequencies using the spec function

```
A = M^-1*K;
[R, diagevals] = spec(A);
disp('Natural frequency (spec) in rad/s:')
cont=0;
for i=1:NTGL
   if diagevals (i,i) ~= 1 && diagevals (i,i) ~= 0
     cont = cont+1;
     disp(sqrt(diagevals (i,i)));
     frequency(cont) = sqrt(diagevals (i,i));
   end
end
```

Source: elaborated by the authors.

4 Results and discussion

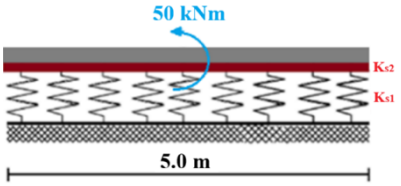
In this section, three dynamic problems of beams on an elastic foundation are presented. These problems are analyzed using the computational code developed in the Scilab environment. The beam materials have a linear elastic constitutive relationship, and structural analyses are assumed under the infinitesimal deformation hypothesis.

4.1 Beam with free ends on an elastic foundation

Consider a beam of finite length and free ends, supported on an elastic foundation and subjected to a concentrated moment of magnitude 50 kNm applied at its center, as per the structural model illustrated in Figure 5. The beam has a length of 5 m and its cross-section has dimensions (0.4 × 1.0) m^2. In this example, the Winkler and Pasternak soil models are considered. The foundation parameter values are: k_{s1} = 3.081 MPa and k_{s2} = 12,449 MN. The beam is made of wood with a longitudinal modulus of elasticity of E = 10.5 GPa and the mass density adopted is ρ = 470 kg/m^3. The beam is discretized into 20 finite elements. Figure 6 presents the deformed configurations of the beam subjected to static loading, considering the Winkler and Pasternak models for representing the foundation. It is observed that the maximum deformations obtained with Pasternak are smaller/lower, which is in agreement with the results presented by Mullapudi and Ayoub (2010).

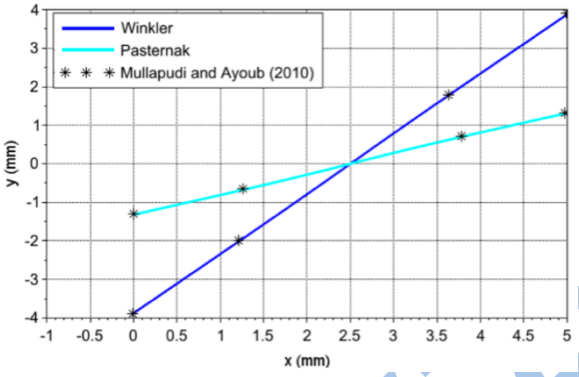
Figure 5 – Structural model of the beam with free ends

Early View



Source: elaborated by the authors.

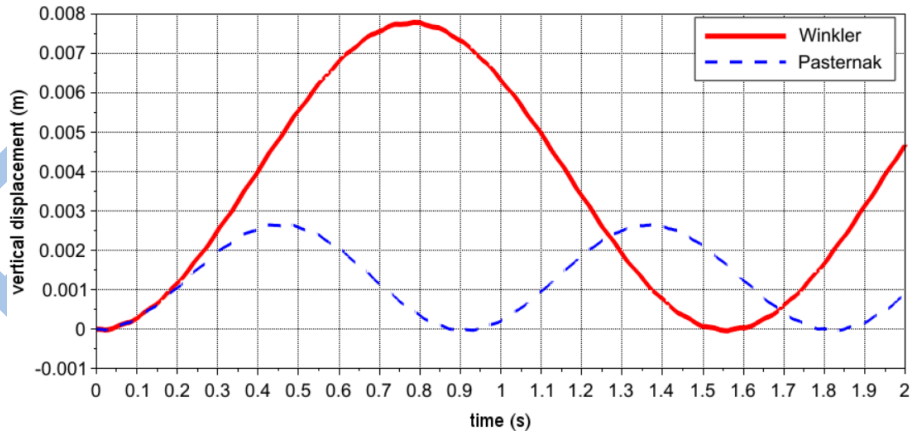
Figure 6 – Deformed configurations of the beam with free ends for the Winkler and Pasternak soil models



Source: elaborated by the authors.

In the transient dynamic analysis (Figure 7), the response of the free end demonstrates the direct influence of the foundation modeling on the vibration characteristics. The dynamic curves are obtained with a time increment $\Delta t = 2.0 \times 10^{-3}$ s and a maximum time $t_{max} = 2$ s. It is observed that, in the Winkler model, the beam exhibits displacements with greater amplitude and a longer oscillation period, indicating a lower effective stiffness. Conversely, in the Pasternak model, the lateral interaction provided by the shear parameter results in oscillations of smaller amplitude and a reduced period. This difference highlights that the foundation coupling contributes to the reduction of the structure's dynamic response, redistributing the vibrational energy more efficiently.

Figure 7 – Transient analysis of the beam with free ends using the Winkler and Pasternak soil models



Source: elaborated by the authors.

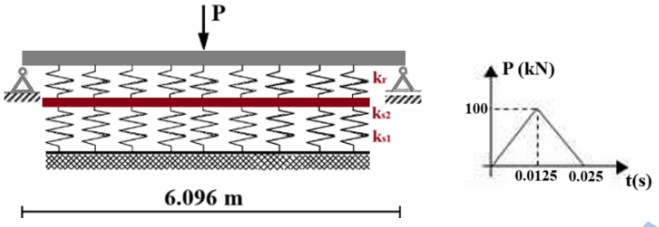
4.2 Simply supported beam on an elastic foundation

Consider a simply supported beam subjected to a time-varying load, as per the structural model illustrated in Figure 8. The geometric and physical properties of this structure are: length $L = 6.096$ m, cross-sectional area $A = 185.81 \times 10^{-3}$ m^2, moment of inertia $I = 1.44 \times 10^{-3}$ m^4, modulus of elasticity $E = 2.483 \times 10^{10}$ Pa, and mass density $\rho = 2{,}400.7319$ kg/m^3. This structure was studied by Rosas, Silva,

Early View

and Silveira (2018), considering the soil represented by the Winkler model (k_{s1} = 16,554 MPa). This problem is adapted here by adding the Pasternak (k_{s1} = 16,554 MPa and k_{s2} = 10,000 kN assuming medium clay) and Kerr (k_{s1} = 16,554 MPa, k_{s2} = 10,000 kN, and k_r = 50,000 kPa for a stiff concrete or high-stiffness mortar layer) soil models to the transient analysis. The structure was discretized using 60 finite elements.

Figure 8 – Structural model of the beam on foundation

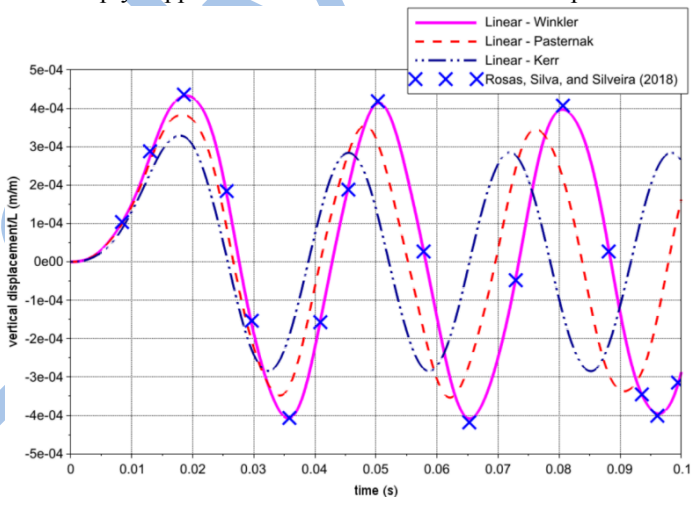


Source: elaborated by the authors.

Figure 9 shows the time versus vertical displacement curves at the beam's center for the different soil models, considering a time increment Δt = 1.0 × 10^{-4} s and a maximum time t_{max} = 0.1 s. Table 1 presents the first three natural frequencies. It is observed that, in the case of the Winkler model, the transient curves presented with the model implemented here show good agreement with those reported by Rosas, Silva, and Silveira (2018), reproducing the expected oscillation pattern and amplitudes.

Regarding the natural frequencies determined in the present study, they show close values to those obtained by the same authors, as shown in Table 1. This proximity confirms the suitability of the numerical formulation and the computational implementation, validating the reliability of the code developed for dynamic analyses of beams on an elastic foundation.

Figure 9 – Simply supported beam: time versus vertical displacement curves



Source: elaborated by the authors.

The transient analysis presented in Figure 9 highlights differences in the dynamic behavior of the simply supported beam depending on the soil model adopted. It is noted that the Winkler model results in greater displacement amplitudes and a longer oscillation period, due to its simplified formulation that considers only the local reaction proportional to displacement. With respect to the Pasternak model, the coupling effect through the shear layer is introduced, which increases the system's effective stiffness and reduces both the amplitude and the period of the oscillations. The Kerr

E-View

model, in turn, exhibits the stiffest response, characterized by smaller displacements and higher vibration frequencies, due to the inclusion of the third stiffness parameter, which represents the presence of an additional stiff layer in the soil.

These trends are confirmed by the natural frequency values listed in Table 1. For all analyzed modes, the frequencies obtained with the Kerr model are higher than those found with the Pasternak and Winkler models, indicating a greater global stiffness of the soil-structure system. The difference is particularly notable in the second mode of vibration, where the natural frequency obtained with the Kerr model ($\omega_2 \cong 83.860367$ Hz) is substantially higher than that of Pasternak ($\omega_2 \cong 61.896348$ Hz) and Winkler ($\omega_2 \cong 56.819529$ Hz). This behavior underscores that the introduction of the third stiffness parameter not only alters the fundamental frequency but also has an increasing influence on the higher modes, reinforcing the sensitivity of the dynamic response to the refinement of the foundation model.

Table 1 – Simply supported beam: the first three natural frequencies (Hz)

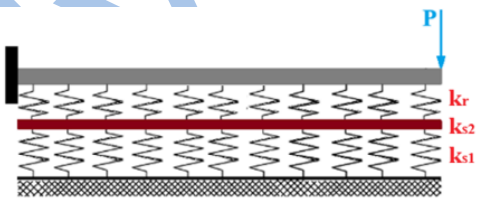
Natural frequencies	Winkler (present study)	Winkler (Rosas; Silva; Silveira, 2018)	Pasternak (present study)	Kerr (present study)
ω_1	32.908454	32.9123	35.124698	37.867787
ω_2	56.819529	56.8499	61.896348	83.860367
ω_3	111.86852	112.0392	117.76710	131.88614

Source: elaborated by the authors.

4.3 Cantilever beam on an elastic foundation

Consider the hypothetical problem of a cantilever beam supported on a foundation with a length equal to 5.0 m, flexural stiffness $EI = 1.0 \times 10^4$ kN m^2, and subjected to a vertical force of magnitude P = 100 kN, according to the structural model illustrated in Figure 10. This structure was statically analyzed by Silva (2004) considering the Winkler soil model. The beam is discretized using ten finite elements and 11 nodes.

Figure 10 – Structural model of the cantilever beam

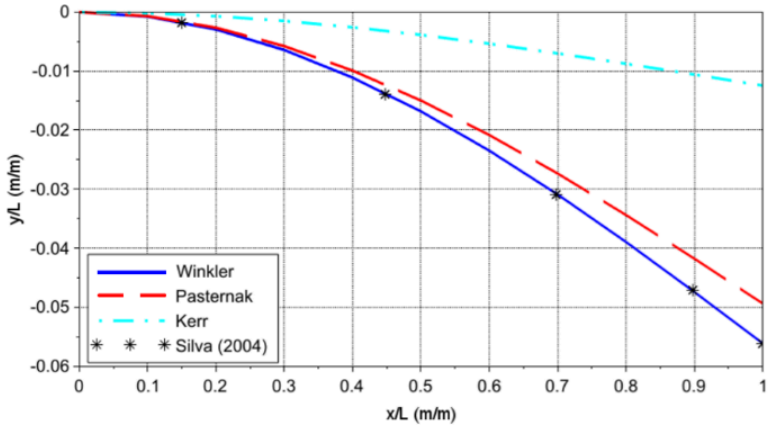


Source: elaborated by the authors.

The static and transient analyses are performed using the three soil models: Winkler (k_{s1} = 100 kPa), Pasternak (k_{s1} = 100 kPa and k_{s2} = 200 kN), and Kerr (k_{s1} = 100 kPa, k_{s2} = 200 kN, and k_r = 50 MPa). Figure 11 shows the deformed configurations of the cantilever beam for the static analysis. The time versus vertical displacement curves at the free end of the beam without and with structural damping are shown in Figures 12 and 13, respectively. The curves from the transient analyses are obtained considering a time increment Δt = 0.01 s for the Backward Acceleration Method. A mass density of ρ = 278.5 kg/m^3 and a damping coefficient of c_m = 0.2 kNs/m were adopted.

Figure 11 – Deformed configurations of the cantilever beam for the soil models

Early View

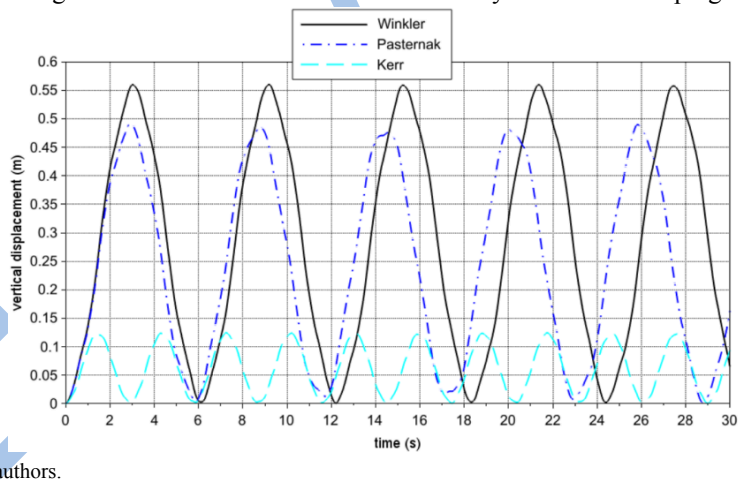


Source: elaborated by the authors.

Regarding Figure 11, the analysis of the deformed configuration of the cantilever beam highlights the direct influence of soil model refinement on the static structural response. It is observed that the Winkler model exhibits the largest vertical displacements at the free end, a behavior attributed to the absence of interaction between adjacent springs, which imparts greater flexibility to the system. Conversely, the Kerr model displays the stiffest response, resulting in the smallest deflections, while the Pasternak model lies in an intermediate position.

The vibration amplitude is inversely related to the stiffness of the structural system for a given load. Since the Kerr model presents the stiffest response, it is physically expected to oscillate with smaller amplitudes compared to the Winkler and Pasternak models, as illustrated in Figure 12. The increased stiffness in the Kerr model also raises the natural frequencies of vibration. Stiffer systems tend to limit motion under dynamic loads more effectively than flexible systems, such as Winkler's, which allow for larger displacement amplitudes and longer oscillation periods.

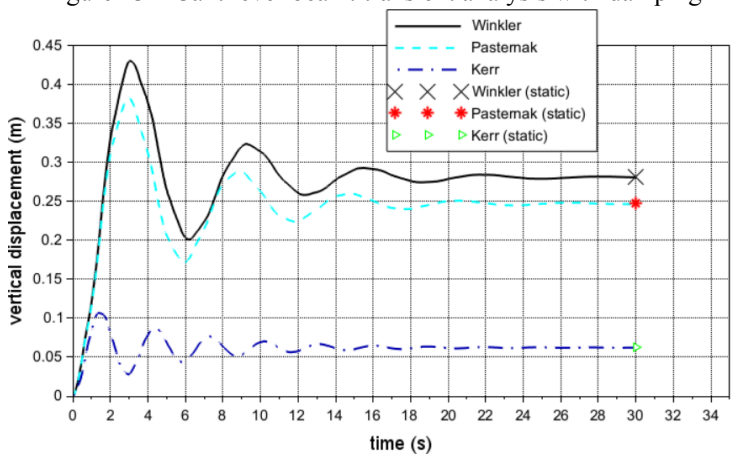
Figure 12 – Cantilever beam: transient analysis without damping



Source: elaborated by the authors.

Early View

Figure 13 – Cantilever beam: transient analysis with damping



Source: elaborated by the authors.

The introduction of damping into the dynamic system plays a fundamental role in verifying the physical consistency of the analyzed models. It is observed in the time response curves (Figure 13) that progressive energy dissipation reduces the amplitude of free oscillations until the system reaches rest. It is noteworthy that, as $t \rightarrow \infty$, the vertical displacement in all soil models converges asymptotically to the exact values obtained in the static analysis (presented in Figure 11). The Winkler model, due to its lower stiffness, exhibits larger oscillation amplitudes and settles at a higher level of deformation. On the other hand, the Kerr model, by incorporating shear stiffness and an additional layer, not only reduces peak amplitudes during the transient regime but also converges to a static equilibrium state with smaller displacements. This direct correlation between the final state of the damped transient regime and the static solution validates the robustness of the time integration algorithm employed, demonstrating that the proposed matrix formulation correctly captures the stiffness, inertia, and energy dissipation mechanisms of the structure.

5 Conclusion

In this article, the explicit formulation of the stiffness matrix for the Kerr soil model was presented, implemented in the context of the Finite Element Method (FEM) for the dynamic analysis of beams on elastic foundations. The methodology employed Euler-Bernoulli beam finite elements with two nodes and four degrees of freedom (DOF), condensed mass matrix, and mass-proportional damping. The equation of motion was solved using the Backward Acceleration Method, ensuring numerical stability, simplicity of implementation, and energy conservation throughout the transient simulations.

The numerical examples studied (the free beam, simply supported beam, and cantilever beam) allowed for the comparison of the Winkler, Pasternak, and Kerr soil models. The results showed that the Winkler model tends to overestimate displacements and underestimate frequencies, while the Pasternak model exhibited higher stiffness due to the lateral coupling (shear layer effect). The Kerr model, in turn, presented the most realistic and stiff response, with lower displacements and higher natural frequencies, capable of capturing the additional effects of stiff layers in the soil. The validation against literature results confirmed the consistency of the formulation and the computational implementation.

However, the numerical model is subject to some limitations, including the assumptions of geometric and material linearity, the use of a lumped mass matrix, and the adoption of idealized bilateral contact. Consequently, the results are valid only within the context of small deformations and linear elastic behavior. Nonlinear effects, such as soil plasticity, stiffness degradation, loss of contact, or large displacement kinematics, are not represented in the present formulation, although they may significantly influence the structural response under higher load levels or cyclic conditions. Therefore,

Early View

the analysis of such phenomena requires more advanced numerical approaches, incorporating nonlinear constitutive models and appropriate solution strategies.

As practical applications, the model can be used in the dynamic analysis of building foundations, railway tracks, pavements, and buried pipelines, in situations where the soil representation exerts a decisive influence on the structural performance. For future research, it is recommended to expand the formulation to consider geometric and material nonlinearities, unilateral contact models, viscoelastic soil effects, and coupling with seismic loads or traffic-induced vibrations, aiming for greater generalization and applicability in real engineering problems.

Acknowledgements

The authors gratefully acknowledge the Federal Technological University of Paraná (UTFPR) for the support in the development of this research.

Funding

This research received no funding.

Conflicts of interest

The authors declare that there are no conflicts of interest.

Author contributions

SOUZA, L. A. F.: conception or design of the study/research; data collection, analysis, and/or interpretation; initial drafting or substantive revision of the manuscript. **SILVA, S. C.:** conception or design of the study/research; data collection, analysis, and/or interpretation; initial drafting or substantive revision of the manuscript.

References

ATTAR, M.; KARRECH, A.; REGENAUER-LIEB, K. Non-linear analysis of beam-like structures on unilateral foundations: A lattice spring model. **International Journal of Solids and Structures**, v. 88-89, p. 192-214, 2016. DOI: https://doi.org/10.1016/j.ijsolstr.2016.03.007.

AVRAMIDIS, I. E.; MORFIDIS, K. Bending of beams on three-parameter elastic foundation. **International Journal of Solids and Structures**, v. 43, n. 2, p. 357-375, 2006. DOI: https://doi.org/10.1016/j.ijsolstr.2005.03.033.

BRITO, W. K. F. **Vigas e placas espessas em base elástica de Kerr**: formulações do método dos elementos de contorno. Tese (Doutorado em Engenharia Civil e Ambiental) – Universidade Federal da Paraíba, João Pessoa, 2024. Disponível em: https://repositorio.ufpb.br/jspui/handle/123456789/32746. Acesso em: 17 Dec. 2025. In Portuguese.

CHEN, Z.; HE, M.; TAO, Y.; YANG, Y. B. An efficient and robust nonlinear dynamic analysis method for framed structures using the rigid body rule. **International Journal of Structural Stability and Dynamics**, v. 22, n. 03n04, 2240001, 2022. DOI: https://doi.org/10.1142/S0219455422400016.

CHOPRA, A. K. **Dynamics of Structures**: Theory and Applications to Earthquake Engineering. 5th. ed. Harlow: Pearson, 2020.

CHUNG, J.; YOO, H. H. Dynamic analysis of a rotating cantilever beam by using the finite element method. **Journal of Sound and Vibration**, v. 249, n. 1, p. 147-164, 2002. DOI: https://doi.org/10.1006/jsvi.2001.3856.

Early View

CIMELLARO, G. P.; MARASCO, S. **Introduction to Dynamics of Structures and Earthquake Engineering**. Cham, Switzerland: Springer, 2018.

CRAIG JR., R. R.; KURDILA, A. J. **Fundamentals of Structural Dynamics**. Hoboken, USA: John Wiley & Sons, 2006.

DAI, Z.-H.; DU, Y.-R.; XU, D.; CHEN, Z.-Y. Calculations of internal forces and rational reinforcement of raft foundation resting on Kerr-equivalent Pasternak ground. **Computers & Structures**, v. 316, 107835, 2025. DOI: https://doi.org/10.1016/j.compstruc.2025.107835.

DASSAULT SYSTEMES. **Scilab**. Version 2025.1.0. Vélizy-Villacoublay: Dassault Systèmes, 2025. Available at: https://www.scilab.org/download/scilab-2025.1.0. Accessed on: 28 Sept. 2026.

FERNANDES, W. L.; VASCONCELLOS, D. B.; GRECO, M. Dynamic instability in shallow arches under transversal forces and plane frames with semirigid connections. **Mathematical Problems in Engineering**, v. 2018, n. 1, 1985907, 2018. DOI: https://doi.org/10.1155/2018/1985907.

GUELLIL, M.; SAIDI, H.; BOURADA, F.; BOUSAHLA, A. A.; TOUNSI, A.; AL-ZAHRANI, M. M.; HUSSAIN, M.; MAHMOUD, S. R. Influences of porosity distributions and boundary conditions on mechanical bending response of functionally graded plates resting on Pasternak foundation. **Steel and Composite Structures**, v. 38, n. 1, p. 1-15, 2021. DOI: https://doi.org/10.12989/scs.2021.38.1.001.

KARKON, M.; KARKON, H. New element formulation for free vibration analysis of Timoshenko beam on Pasternak elastic foundation. **Asian Journal of Civil Engineering (BHRC)**, v. 17, n. 4, p. 427-442, 2016. Available at: https://www.sid.ir/en/VEWSSID/J_pdf/103820160403.pdf. Accessed on: 28 Sept. 2026.

KERR, A. D. A study of a new foundation model. **Acta Mechanica**, v. 1, n. 2, p. 135-147, 1965. Available at: https://link.springer.com/article/10.1007/BF01174308. Accessed on: 28 Sept. 2026.

KWON, Y. W.; BANG, H. **The finite element method using MATLAB**. 2nd. ed. Boca Raton, USA: CRC Press, 2018.

LIMKATANYU, S.; KUNTIYAWICHAI, K.; SPACONE, E.; KWON, M. Nonlinear Winkler-based beam element with improved displacement shape functions. **KSCE Journal of Civil Engineering**, v. 17, n. 1, p. 192-201, 2013. DOI: https://doi.org/10.1007/s12205-013-1606-0.

LIU, T. Y.; LI, Q. B.; ZHAO, C. B. An efficient time-integration method for nonlinear dynamic analysis of solids and structures. **Science China Physics, Mechanics and Astronomy**, v. 56, n. 4, p. 798-804, 2013. DOI: https://doi.org/10.1007/s11433-013-5021-9.

MOURYA, V. K.; PANDEY, G.; PATEL, D.; KUMAR, R. Approaches considering non-linearity in soil-foundation-interaction: a state-of-the-art review. **Research on Engineering Structures & Materials**, v. 9, n. 3, p. 989-1013, 2023. DOI: http://dx.doi.org/10.17515/resm2023.646me0117.

MULLAPUDI, R.; AYOUB, A. Nonlinear finite element modeling of beams on two-parameter foundations. **Computers and Geotechnics**, v. 37, n. 3, p. 334-342, 2010. DOI: https://doi.org/10.1016/j.compgeo.2009.11.006.

Early View

PANDEY, G.; PATEL, D.; MOURYA, V. K.; KUMAR, R.; KUMAR, S. A review on soil-foundation-interaction models. **Journal of Rehabilitation in Civil Engineering**, v. 11, n. 3, p. 158-179, 2023. DOI: https://doi.org/10.22075/jrce.2022.25247.1570.

PASTERNAK, P. L. On a new method of analysis of an elastic foundation by means of two foundation constants. **Gosudarstvennoe Izdatelstvo Literaturi po Stroitelstuve i Arkhitekture**, 1954. Available at: https://cir.nii.ac.jp/crid/1570009750158012032. Accessed on: 28 Sept. 2026.

ROSAS, L.; SILVA, A.; SILVEIRA, R. Nonlinear dynamic analysis of structures in contact with soil. **Revista Internacional de Métodos Numéricos para Cálculo y Diseño en Ingeniería**, v. 34, n. 1, p. 1-14, 2018. DOI: https://doi.org/10.23967/j.rimni.2017.9.001.

SILVA, L. F. **Cálculo dos esforços internos e deflexões de vigas sobre a base elástica não linear usando o método da flexibilidade**. 2004. Dissertação (Mestrado em Engenharia Civil) – Escola de Minas, Universidade Federal de Ouro Preto, Ouro Preto, 2004. Disponível em: http://www.repositorio.ufop.br/handle/123456789/6312. Acesso em: 20 Mar. 2026. In Portuguese.

SILVEIRA, R. A. M.; PEREIRA, W. L. A.; GONÇALVES, P. B. Nonlinear analysis of structural elements under unilateral contact constraints by a Ritz type approach. **International Journal of Solids and Structures**, v. 45, n. 9, p. 2629-2650, 2008. DOI: https://doi.org/10.1016/j.ijsolstr.2007.12.012.

SORIANO, H. L. **Introdução à dinâmica das estruturas**. Rio de Janeiro: Elsevier, 2014. In Portuguese.

SOUZA, L. A. F. Modelo numérico-computacional para a análise modal e transiente de *shear building* utilizando o programa Scilab. **Revista Brasileira de Ensino de Física**, v. 46, e20240014, 2024. DOI: https://doi.org/10.1590/1806-9126-RBEF-2024-0014. In Portuguese.

TEODORU, I.-B.; MUŞAT, V. Beam elements on linear variable two-parameter elastic foundation. **Buletinul Institutului Politehnic din Iasi. Sectia Constructii, Arhitectura**, v. 54, n. 2, p. 69-78, 2008. Available at: https://www.proquest.com/openview/245f01c642653f5d1691ec7d3cf9fbeb/1?pq-origsite=gscholar&cbl=55208. Accessed on: 28 Aug. 2026.

WANG, Y.-N; ZHOU, H.-Z; WANG, L.-C. Settlement mode analysis for an immersed tube tunnel considering a nonuniform foundation under tidal load. **China Ocean Engineering**, v. 36, n. 3, p. 427-438, 2022. DOI: https://doi.org/10.1007/s13344-022-0038-3.

WORKU, A.; HABTE, B. Analytical formulation and finite-element implementation technique of a rigorous two-parameter foundation model to beams on elastic foundations. **Geomechanics and Geoengineering**, v. 17, n. 2, p. 547-560, 2022. DOI: https://doi.org/10.1080/17486025.2020.1827162.

YOUNESIAN, D.; HOSSEINKHANI, A.; ASKARI, H.; ESMAILZADEH, E. Elastic and viscoelastic foundations: a review on linear and nonlinear vibration modeling and applications. **Nonlinear Dynamics**, v. 97, n. 1, p. 853-895, 2019. DOI: https://doi.org/10.1007/s11071-019-04977-9.

Early View